Article

Biomass Combustion in Boiler: Environmental Monitoring of Sugar Markers and Pollutants

Enrico Paris [1], Monica Carnevale [1,*], Adriano Palma [1], Beatrice Vincenti [1], Mariangela Salerno [1], Andrea Rosario Proto [2], Salvatore Papandrea [2], Ettore Guerriero [3], Mattia Perilli [3], Marina Cerasa [3], Valerio Di Stefano [4] and Francesco Gallucci [1,3]

[1] Consiglio per la Ricerca in Agricoltura e L'analisi Dell'economia Agraria (CREA), Centro di Ricerca Ingegneria e Trasformazioni Agroalimentari, Via Della Pascolare 16, 00015 Monterotondo, Italy; enrico.paris@crea.gov.it (E.P.); beatrice.vincenti@crea.gov.it (B.V.); mariangela.salerno@crea.gov.it (M.S.); francesco.gallucci@crea.gov.it (F.G.)

[2] Department of Agraria, University of Reggio Calabria, 89122 Reggio Calabria, Italy; andrea.proto@unirc.it (A.R.P.); salvatore.papandrea@unirc.it (S.P.)

[3] National Research Council of Italy, Institute of Atmospheric Pollution Research (CNR-IIA), Via Salaria km 29,300, 00015 Monterotondo, Italy; guerriero@iia.cnr.it (E.G.); perilli@iia.cnr.it (M.P.); marina.cerasa@cnr.it (M.C.)

[4] Consiglio per la Ricerca in Agricoltura e L'analisi Dell'economia Agraria (CREA), Centro di Centro di Ricerca Foreste e Legno, 00184 Rome, Italy; valerio.distefano@crea.gov.it

* Correspondence: monica.carnevale@crea.gov.it

Abstract: The need to use renewable sources and matrices with energy potential is widely recognized. The development of innovative technologies aimed at the improvement of energy conversion processes and reducing environmental impacts is currently receiving increasing attention from the scientific community and policymakers. The presence of sugars in airborne particle materials is attributed to biomass combustion. For this reason, these compounds are considered markers of biomass burning. The purpose of this work was to evaluate the emissions produced by agroforestry biomass burning (citrus pruning) by simultaneously sampling both stack emissions and atmospheric particulates in the area around a biomass boiler to understand the real contribution of biomass burning to atmospheric pollution. The combustion tests were carried out by comparing the processes with and without particulate abatement system to see how biomass combustion's contribution to particulate emission can be controlled and reduced. During the tests, the focus was on particulate matter (PM) speciation in terms of sugar marker identification and determination. This study aims to increase knowledge to better understand the contribution of biomass plants to air pollution and differentiate it from the contributions of other sources, such as vehicular traffic or domestic heating.

Keywords: air pollution; PM; VOC; sugar; bioenergy; biomass disposal; biomass burning

1. Introduction

The growing demand for renewable energies has encouraged the installation of many small-scale power plants using wood waste as combustion feedstock [1]. There are many studies concerning the importance of biomass burning (BB) despite its relative atmospheric impact [2,3].

BB represents a significant source of pollutants that enter into the atmosphere [4–6], such as particulate matter (PM), volatile organic compounds (VOCs), polycyclic aromatic hydrocarbons (PAHs), macropollutants (CO, CO_2, NO_x, SO_2) [7–9]. These compounds can potentially impact and have important consequences for human health, the climate, biogeochemical cycles, ecosystems, and global radiation balance [10–12].

The emissions generated by BB strongly influence the physical and chemical composition of atmospheric aerosols, especially in cases of uncontrolled wood combustion (open burning), which, unfortunately, is still frequently used as a waste disposal method in

rural areas [2,13]. Numerous other studies have investigated the influence of BB emissions on atmospheric aerosol compositions [14–18]. This practice is responsible for one third to one half of global carbon monoxide (CO) emissions and 20% of nitrogen oxide (NO_x) emissions [19]. BB also represents the main source of primary fine carbonaceous particles and the second largest source of trace gases in the global atmosphere [20,21]. Emissions from BB have differ greatly based on the process dynamics, nature of the biomass, and the abatement system and can be a result of incomplete combustion. Incomplete combustion mostly produces soot, organic micropollutants, unburnt carbon, ash, and carbon monoxide. Under bad combustion conditions, the percentage of unburnt particles can reach more than 90% of the total particles, while the percentage is less than 1% if the best combustion condition is reached [22]. Recent studies show that fossil charcoal and black carbon, derived from the incomplete combustion of plants, are the tracers of forest fires [23–25]. The use of biomass boilers allows us to burn biomass in controlled conditions to produce energy and reduce the environmental impact of BB.

Levoglucosan is universally recognized as a specific molecular marker of biomass combustion. This monosaccharide is produced from the thermal degradation of cellulose during the pyrolysis phase at 300 °C by transglycosylation and fission reactions and subsequently emitted in particulate matter [26–28]. Levoglucosan is considered [29] relatively stable in atmosphere, being emitted in large amounts [30], and it is usually preferred to soluble potassium as a specific tracer, since the latter has other sources, such as meat cooking, waste incineration, and coal usage [31].

Based on the several published studies investigating the presence of levoglucosan in the atmosphere, it appears that the most commonly used techniques for its detection are HPLC/MS [32] or HPLC coupled with an amperometric detector [26,33,34]. More recent studies have proposed other innovative techniques, such as thermal desorption coupled with gas chromatography mass spectrometry (TD-GC/MS) with in situ derivatization [35]. Levoglucosan is generally observed in atmospheric monitoring stations, and its presence is usually attributed to all biomass combustion, both industrial and, above all, domestic [36]. Indeed, this marker sugar is also derived from other phenomena (forest fires; the use of domestic fireplace; the burning of stubble and pruning the so-called open burning, a practice that is still sadly widespread; etc.), which led to an overestimation of the PM generated by biomass boilers [36]. The described phenomena are in fact devoid of abatement systems (unlike boilers) and therefore lead to overestimates of the amount of PM from biomass conversion plants. The aim of this work was to monitor, by sampling and analysis, emissions from biomass conversion processes and their contribution to the composition of atmospheric PM. Also, this work aimed to determine the main sugars generated by BB through dedicated sampling methods to identify the characteristic patterns that uniquely define the controlled combustion impact. Unlike other works in the literature, here, for the first time, the volatile fractions of sugars, determined by a method previously proposed by the authors of [36], are also considered. The proposed work consisted of three monitoring and analysis phases:

- The chemical and physical characterization of incoming biomass;
- The combustion and stack monitoring of CO, CO_2, NO_x, SO_2, TOC, PM, PM_{10}, $PM_{2.5}$, metals, VOC, and sugars;
- The sampling and analysis of environmental PM.

A further innovation proposed in this work is the fact that we chose to conduct the proposed analyses in two different boiler operating conditions: with and without the multicyclonic filter. This allowed us to obtain significant results that also show the differences between the emissions of a controlled combustion and a combustion that simulates the open burning phenomena. Although the use of biomass in thermochemical processes is an excellent system for disposal and the production of renewable energy, it is necessary to deepen our understanding of the impact that uncontrolled and controlled combustion processes can have on the atmosphere. This paper helps bridge a gap in global biomass utilization knowledge.

2. Materials and Methods

2.1. Biomass Composition

To evaluate the emissions produced, it is important to observe the parameters and operative conditions of the combustion plant, the combustion process, and the physical and chemical characterization of biomass (moisture content, ash content, particle size, and elemental content) [37,38]. The biomass (pruning of citrus trees) was shredded and dried to reduce its size and humidity, thus facilitating characterization. The moisture content was determined using a Memmert UFP800 oven according to the ISO 18134-1:2022 (Solid biofuels—Determination of moisture content. International Organization for Standardization. Geneva, Switzerland) standard. In particular, the biomass sample was dried at 105 ± 2 °C, and the moisture content was calculated considering the weight loss of the sample due to the drying process after 24 h. For the ash content test, the dried sample was first ground with the Retsch SM 100 knife mill for preliminary size reduction and then put through the Retsch ZM 200 centrifugal mill. The ash content was determined using a muffle furnace Lenton EF11/8B according to the ISO 18122:2023 (Solid biofuels—Determination of ash content. International Organization for Standardization. Geneva, Switzerland). A sample of about 1 g was placed in a ceramic crucible and then placed in the oven. The oven temperature was set with two different temperature ramps relating to two steps: the first was up to 250 °C for one hour at 6 °C/min, and the second was from 250 °C to 550 °C for two hours at 10 °C/min. For the evaluation of the chemical and energy parameters, the higher heating value (HHV); lower heating value (LHV); and carbon (C), hydrogen (H), nitrogen (N), and sulfur (S) contents were determined. The HHV was determined using the Parr 6400 calorimeter according to the ISO 18125:2017 (Solid biofuels—Determination of calorific value. International Organization for Standardization. Geneva, Switzerland). The LHV was calculated by applying an algorithm, starting from the HHV value [39].

$$LHV = HHV - (206 \times H/1000)$$

The elemental composition in terms of C, H, and N, was determined using a Costech ECS 4010 CHNS-O elemental analyzer according to the ISO 16948:2015 (Solid biofuels—Determination of total content of carbon, hydrogen and nitrogen. International Organization for Standardization. Geneva, Switzerland).

2.2. Experimental Tests and Biomass Combustion Plant

The combustion tests and the emission monitoring campaigns were carried out in two sites: CREA-IT and ARSAC. At CREA-IT, in Monterotondo (Rome, Italy), combustion was carried out by means of an 80 kW$_{th}$ boiler (GSA/80, D'Alessandro Termomeccanica. Miglianico, Italy) without abatement systems to simulate *open burning* conditions. The biomass was conveyed in the upper auger; the star valve served to regulate the supply chain of the fuel towards the cochlea and break the continuity of the fuel, preventing the return of any flames. In the ARSAC site, in San Marco Argentano (Cosenza, Italy), the biomass was burned into a 30 kW$_{th}$ boiler equipped with a multicyclone for collecting fly ash to perform the combustion process under controlled conditions with abatement systems (CSA 30–100 GM, D'Alessandro Termomeccanica. Miglianico, Italy). The boiler we used is a hydronic (i.e., it uses water as a heat transfer medium), single-fuel boiler that is able to consume 7.1 kg/h of combustible at max work condition. The feeding system allowed for the use of solid biomass such as woodchips and crushed wood waste [40]. The two systems' operative parameters, detected using an isokinetic probe, are reported in Table 1.

Table 1. Experimental conditions and operative parameters of the two processes.

Sampling and Combustion Conditions		
	Open Burning Simulation	Boiler with Abatement System
Flue gas velocity at stack [m/s]	3.60	3.35
Stack temperature [°C]	218.52	142.46

Table 1. *Cont.*

Sampling and Combustion Conditions		
	Open Burning Simulation	**Boiler with Abatement System**
Stack pressure [kPa]	102.96	110.96
Velocity at nozzle [m/s]	3.567	3.353
Filter box temperature [°C]	130.7	129.8
Outlet temperature [°C]	99.3	95.6
Ambient pressure [kPa]	102.86	100.98

2.3. Emission Sampling and Characterization

Emission sampling and determination was carried out following the ISO 16911-1:2013 (Stationary source emissions—Manual and automatic determination of velocity and volume flow rate in ducts—Part 1: Manual reference method. International Organization for Standardization. Geneva, Switzerland) and UNI EN 13284:2017 (Emissions from fixed sources—Determination of the mass concentration of dust in low concentrations—Part 1: Manual gravimetric method. Ente italiano di normazione. Milano, Italy). Sugars, metals, and VOCs were also sampled and characterized in the LASER-B laboratory of CREA-IT. At the same time as when the emission monitoring campaign was being carried out at the ARSAC site, the atmospheric concentrations of PM, metals, and sugars were evaluated. For this purpose, 4 Skypost Tecora environmental samples were used for PM_{10} (A, B, C, and D). Points A (north), B (east), C (south), and D (west) were positioned as shown in Figure 1. Furthermore, the use of continuous samplers for the whole campaign duration (three days) made it possible to observe the variations in PM, even when the boiler was switched off.

Figure 1. Positioning of Skypost Tecora samplers during sampling campaign at the ARSAC site in San Marco Argentano (CS). (A) North; (B) east; (C) south; (D) west.

Daily sampling of PM_{10} was carried out following the UNI EN 12341:2014 (Ambient air—Gravimetric reference method for the determination of the mass concentration of suspended particulate matter PM_{10} or $PM_{2.5}$. Ente italiano di normazione. Milano, Italy). For this purpose, was used a PM_{10} autosampler (Skypost TCR Tecora, Cogliate, Italy) at a flow rate of 2.3 m^3/h (Figure 2). The PTFE filters (47 mm diameter) were preconditioned at

a controlled temperature and humidity (48 h at 20 °C and 50% humidity) in a hood with an ionizing system (Climatic Cabinet, Hannover, Germany) to reduce electrostatic charges. For gravimetric analysis, the filters were weighed before and after sampling using an electronic microanalytical balance (Sartorius, Gottingen, Germany) with an accuracy of 0.001 mg, and each weighing was averaged over five repetitions.

Figure 2. PM_{10} environmental sampler (Skypost Tecora) Position B.

2.3.1. Sampling and Determination of Macropollutants

Gaseous macropollutant determination was carried out according to UNI EN 14791 (Emissions from fixed sources—Determination of the mass concentration of sulfur oxides—Standardized reference method. Ente italiano di normazione. Milano, Italy), 14792 (Emissions from fixed sources—Determination of the mass concentration of nitrogen oxides—Standardized reference method: chemiluminescence. Ente italiano di normazione. Milano, Italy) and 15058 (Emissions from fixed sources—Determination of the mass concentration of carbon monoxide (CO)—Reference method: non-dispersive infrared spectrometry. Ente italiano di normazione. Milano, Italy). The flue gas sampling system consisted of two 180 °C line heaters connected to the boiler's stack and two gas analyzers: a Ratfisch model RS 53-T heated flame ionization detector (FID) for the detection of TOC (Total Organic Carbon) and a multiparametric analyzer (Horiba PG250) for the detection of NO_x, SO_2, CO_2, CO, and O_2. Flue gas sampling was carried out with a HP1 (DADO LAB Cinisello B., Milano, Italy) heated sampling probe with a PTFE filter. A chiller was placed between the probe and the Horiba PG 250 to avoid the condensation of the gaseous effluents.

2.3.2. Sampling and Determination of Volatile Organic Compounds (VOCs)

Volatile organic compounds were sampled according to the CEN/TS 13649:2014 standard, applying a dilution with zero air equal to 1/10 thanks to the use of the Dynamic Dilution Sampler for VOC Emission Sampling (DDS TCR Tecora, Cogliate, Italy). The samplings were performed using a heated probe and a self-made adsorbent tube in Activated Porous Carbon Fiber (APCF Labtech SRL, Rome, Italy) [41,42] placed downstream and followed in series by a backup tube. VOC sampling was performed simultaneously with the measurement of the Total Organic Carbon (TOC). The adsorbent tubes were subsequently thermally desorbed and analyzed using a TD-100xr (Markes Int. Bridgent, Wales, UK) coupled with the Agilent 7000 triple quadrupole GC/MS system (Santa Clara, CA, USA). GC/MS analysis was performed in splitless mode with the parameters specified in Table 2.

Table 2. Optimized parameters for the analysis of VOCs in GC/MS.

Operative Parameters	
Carrier gas	He
Column	DB 502.2
Flow	1.2 mL/min
Mode (GC)	Constant Flow
Oven ramp	35 °C (5 min) + 5 °C/min to 230 (5 min)
Ion source	EI
Inlet	200 °C
MS source	230 °C
MSD transfer line	240 °C
Mode (MS)	Full Scan 35–450 m/z

2.3.3. Methods for Sampling and Determining Fixed-Source Sugars

The use of the isokinetic sampling system was followed by the use of impinger systems to collect both the solid fraction and the volatile fraction (Figure 3). Only the solution in the first two impingers were considered for determination; the third was defined as a backup that was exclusively used to validate the sampling: if the analyte investigated exceeds 10% in concentration compared to the sum of the concentration in the first two impingers, the sampling is not considered valid. The impingers were filled with different solutions depending on the sampling. A MilliQ water solution was used to sample the sugars, while a solution of HNO_3 and H_2O_2 in milliQ water was used to sample the metals (method: UNI EN 14385:2004. Emissions from fixed sources—Determination of the total emission of As, Cd, Cr, Co, Cu, Mn, Ni, Pb, Sb, Tl and V. Ente italiano di normazione. Milano, Italy).

Figure 3. Sugar sampling system: DADOLAB HP5 probe containing the fiber glass filter for the solid component and the thermostated impingers for the sampling of the volatile fraction.

PM sampling made it possible to collect the Total Suspended Particles (TSPs) and PM fractions (PM_{10}, $PM_{10-2.5}$, $PM_{2.5}$). TSP sampling was carried out by using an isokinetic probe ST5 DADO LAB according to UNI EN 13284-1:2017 and subsequently determining the quantity in ng/Nm^3 present in the fumes by a gravimetric method. The use of a new prototype of an inertial impactor developed by DADO LAB (Figure 4) in compliance with ISO 23210:2009 (Stationary source emissions Determination of $PM_{10}/PM_{2.5}$ mass concentration in flue gas Measurement at low concentrations by use of impactors. International Organization for Standardization. Geneva, Switzerland) allowed us to sample the three different fractions of PM.

Figure 4. Multistage inertial impactor for PM fraction sampling.

For the determination of PM and sugars, glass fiber filters (47 mm diameter) were conditioned at 400 °C and subsequently brought to a constant weight by keeping them for 48 h at constant temperature and humidity in the conditioning chamber. After sampling, the filters were reweighed and compared with a blank filter. For sugar determination, in accordance with Paris et al. [36], the filters and the impingers, kept in the dark and refrigerated, were analyzed by Ionic Chromatography (IC) using the 945 Professional Vario Amperometric Detector. The impinger solutions were directly analyzed, while the particulate was extracted three times with 1 mL H_2O MQ using an ultrasonic bath for 30 min in three cycles. The separation of the single sugars was carried out out using a Metrosep Carb 2-250/4.0 analytical column, the relative pre-column, and the trap for carbonates (Metrosep CO_3 Trap 1-100/4.0). The mobile phase was an aqueous solution of 18 mM sodium hydroxide (NaOH). The chromatographic run was conducted at a flow rate of 0.8 mL/min. The calibration lines were made using standard sugars with a degree of purity over 99% (Labmix24- Hamminkeln. Germany). Finally, as we knew the sampling volumes of the fumes that have passed through the filter and impingers, it was possible to obtain the emission values of every sugar detected by IC. Figure 5 shows a chromatogram of the construction of the calibration line:
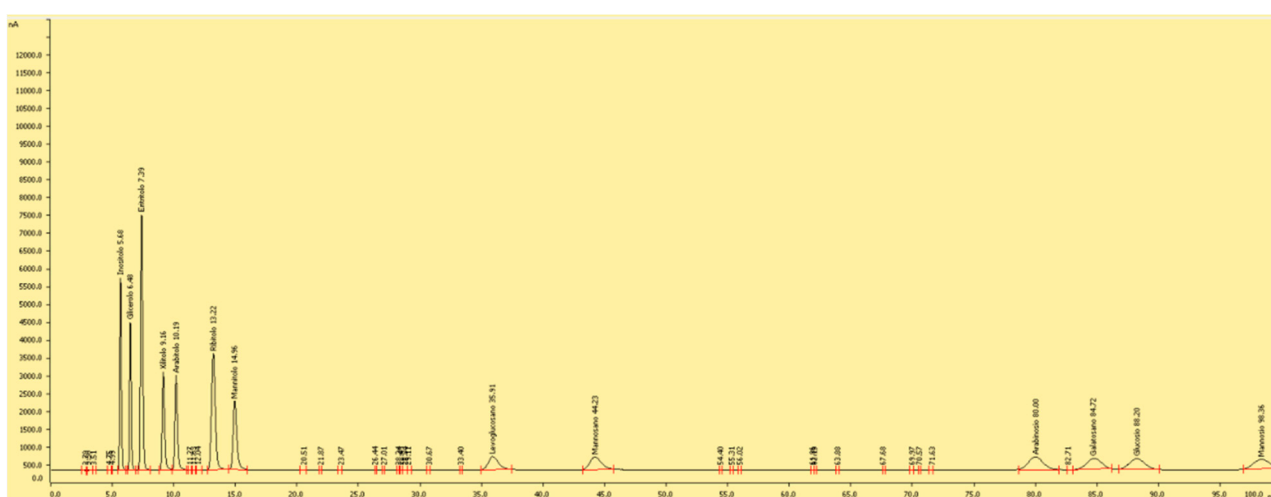

Figure 5. Chromatogram of the standard solution of the main sugars.

2.3.4. Sampling and Determination of Metals

For metal sampling, quartz filters and impingers were used during the sampling campaign. We used impingers containing a 1:1 solution of H_2O_2 at 30% *v/v* and HNO_3

at 65% v/v diluted with 1:10 H_2O MilliQ following the same system for the isokinetic sampling according to the EN 14385:2004. The sampled filters were mineralized with a microwave (Milestone START D. Sorisole, Italy), and the impinger solution was diluted to 1:10. Then, the solutions were analyzed in the ICP-MS 7700 Agilent (Santa Clara, CA, USA) according to UNI EN ISO 17294-2:2016 (Water quality—Application of inductively coupled plasma mass spectrometry (ICP-MS)—Part 2: Determination of selected elements, including uranium isotopes. Ente italiano di normazione. Milano, Italy).

3. Results and Discussion

3.1. Biomass Characterization

The biomass characterization results about the moisture and other parameters that represent important factors for the dynamics and efficiency of the processes are listed in Table 3 [17,40,43,44]. A non-negligible concentration of water and ash was determined; these factors inevitably lead to worse combustion conditions [45]. As regards the metal contents, a high concentration of Na, Mg, K, and Ca was observed. These metal compounds are commonly present in large quantities in woody biomass because they represent the main ionic species in soil absorbed in the growing biomass phase. Ca, Mg, K, and Na oxalates are typical minerals of plants [46]. These bio-minerals are end products of plant metabolism and commonly present in cytoplasm [47]. It is also known that annual and fast-growing crops, including fruit crops, show high contents of elements such as K, Mg, Na, and Ca [46]. For other metals, the concentrations are all below mg/kg, except for Fe and Sr. Their presence is probably due to the type of soil in which the citrus was cultivated.

Table 3. Chemical and physical characterization of biomass.

	Citrus Pruning
Moisture content %	10.19
Ash %	4.95
HHV [MJ/kg]	17.75
LHV [MJ/kg]	16.59
C %	46.69
H %	5.58
N %	0.44
Metal content [mg/kg]	
Na	13.33
Mg	21.73
Al	6.28
K	239.82
Ca	155.01
Cr	0.03
Mn	0.24
Fe	3.97
Ni	0.06
Cu	0.21
Zn	0.25
Ga	0.05
Sr	5.39
Ag	0.001
Cd	0.001
In	0.0004
Ba	0.91
Tl	0.001
Pb	0.01
Bi	0.02

3.2. Emission Characterization

3.2.1. Macropollutant Emissions

The data concerning the emission production were monitored, and the average values of the macropollutants (CO, NO_x, SO_2, CO_2, and TOC) recorded during the combustion process are shown in Table 4. The results were normalized to a 6% oxygen content, in compliance with the Italian Legislative Decree 183/17 about the limits for boiler emissions from biomass burning.

Table 4. Concentrations of macropollutants in emission.

Compound	Open Burning Test	Boiler with Abatement System
CO [mg/Nm^3]	1132.418	587.88
NO_x [mg/Nm^3]	528.12	473.70
SO_2 [mg/Nm^3]	38.03	39.76
TOC [mg/Nm^3]	35.26	47.19
CO_2 [%]	6.55	4.62

Observing Table 4, in the two types of tests, the only value identical in both cases is SO_2, whose formation depends exclusively on the sulfur present in the biomass, which is present in very low concentrations (<LOQ).

A large divergence in CO concentrations is observed, with the CO concentration being almost double in the case of the open burning tests. This is a symptom of low-grade combustion with an uneven or insufficient intake of oxidizer. Although the NO_x amounts are similar, they are slightly higher in the case of the open burning tests, which probably indicates that, in this case, higher temperatures have been reached, which favor the production of this pollutant [48].

3.2.2. VOC Emission

The analysis of the adsorbed tubes through active sampling at the stack highlighted the presence of numerous VOCs (Table 5). In this paper, only the main compounds are reported, with a pick area of at least 5% compared to the highest one or present in the analytical standard.

Table 5. VOCs in emissions.

VOCs [mg/Nm^3]	Open Burning	Boiler with Abatement System
Propene	0.72	0.21
Methane, chloro-	1.03	2.11
Methane, dimethoxy-	0.02	<LOQ
2-Butanone	<LOQ	<LOQ
Benzene	4.13	1.75
Toluene	0.57	0.48
Benzene, chloro-1	0.10	0.05
Ethylbenzene	0.11	0.03
m,p-Xylene	0.22	0.21
o-Xylene	0.08	0.18
D-Limonene	0.26	0.09
Undecane	0.55	0.47
Cyclododecane	0.82	0.20
$\sum_{VOC}$	8.61	5.78

Combustion in a boiler with an abatement system generally produced lower VOC concentrations (the only exception is chloromethane, whose concentration is considerably lower in the open burning emission). The lower VOC concentrations could be due to two reasons:

-   The best combustion conditions (Table 4) resulting in a lower probability of incomplete combustion products production (including VOC).
-   Some of the produced VOCs adsorb at the PM which is captured by the multicyclone.

3.2.3. Sugar Emission

As regards sugar analysis, the calibration line was made using standards of the main sugar typically found in emissions produced by BB based on literature data [26,33,34,49–52]. Table 6 reports the analytes detected in the PM filter, MilliQ H_2O impinger, and backup impinger (Dadolab srl. Cinisello B. Mialno, Italy).

Table 6. Sugar in emissions while under open burning conditions and using multicylone filter.

[mg/Nm^3]	Open Burning			Boiler with Abatement System		
	Filter	**Impinger**	**Backup**	**Filter**	**Impinger**	**Backup**
Inositol	1.11	0.16	<LOQ	1.12	0.32	<LOQ
Glycerol	<LOQ	13.46	1.58	<LOQ	3.47	0.09
Erythritol	2.06	0.07	<LOQ	<LOQ	<LOQ	<LOQ
Ribitol	<LOQ	0.55	<LOQ	<LOQ	<LOQ	<LOQ
Mannitol	1.47	1.27	<LOQ	<LOQ	<LOQ	<LOQ
Levoglucosan	11.23	29.03	<LOQ	3.52	5.91	<LOQ
Mannosan	1.14	1.1	<LOQ	1.05	0.80	<LOQ
Arabinose	6.74	4.55	<LOQ	<LOQ	<LOQ	<LOQ
Arabitol	0.99	0.69	<LOQ	<LOQ	<LOQ	<LOQ

In open burning conditions, inositol, erythritol, mannitol, levoglucosan, mannosan, arabinose, and arabitol were detected in both the PM filter and the impingers. The impingers were particularly rich in sugars, suggesting that in addition to levoglucosan, the high volatility is also typical of other sugars generated by biomass combustion. In tests where a multicyclonic abatement system was used, the results obtained were very different and showed the determination of only four sugars (inositol, glycerol, levoglucosan, and mannosan). In addition to levoglucosan, one of the main analytes detected was glycerol, both in the filter and in the bubbled fractions. Another important parameter that can be seen is the extreme volatility of glycerol. In both cases, in fact, it did not settle on a filter but was determined exclusively in the volatile fraction. Excluding levoglucosan and mannosan, the others all belong to the category of sugar alcohols. These data particularly indicate that abatement systems avoid an enrichment of PM sugars (Figures 6 and 7), and therefore, it is possible to distinguish the PM obtained from boilers with dedicated abatement systems, as well as the PM obtained from the open burning process.
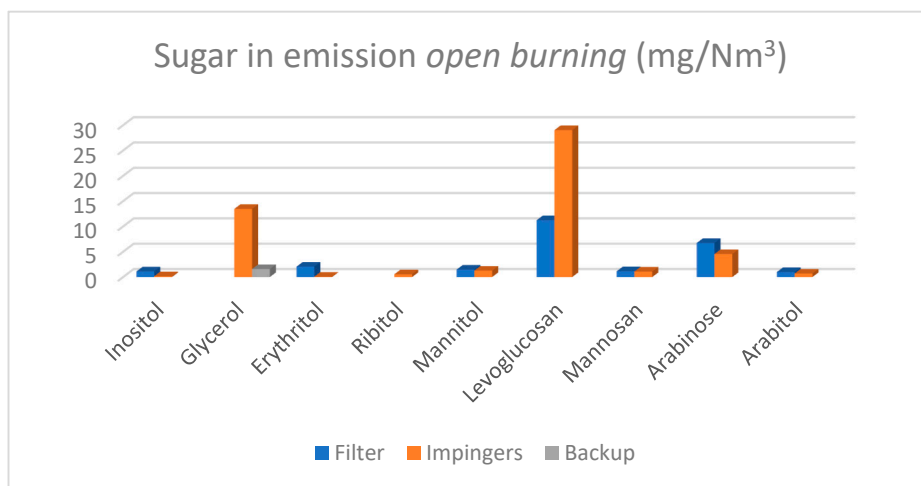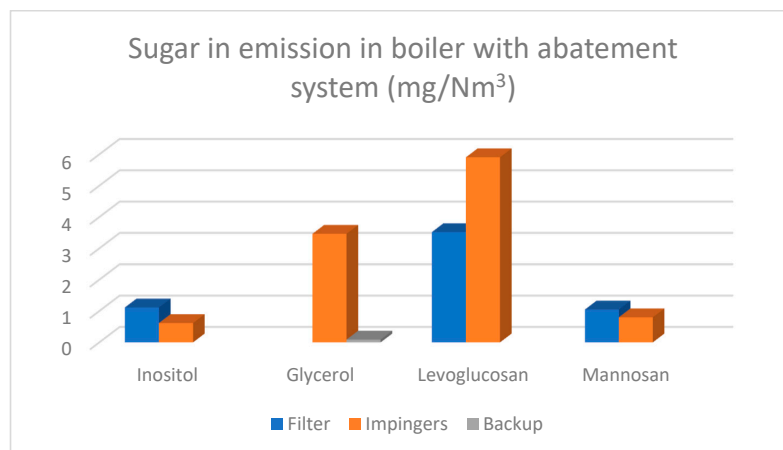

Figure 6. Sugar distribution.

Figure 7. Comparison of sugar distribution in boiler with multicyclone filter.

The determined data allow us to make some important considerations: First of all, the volatile fraction (that is, the one that can be sampled only by the bubbling of the fumes) represents a not negligible fraction of sugars and, therefore, simple filter sampling, often performed in similar works in the literature, is not enough because it greatly underestimates the real contribution of markers to the PM. Moreover, through comparing an uncontrolled combustion process and one with a multi cyclonic abatement system, it can be deduced that the latter, being an effective system in breaking down only relatively large particle material (the abatement efficiency drops dramatically for particles below 5 microns), allows us to subtract a large part of the particle material that is usually released into the atmosphere and to adhere and trap even sugars of reduced size during the swirling motion of abatement. The quantification of sugars on the outdoor samplers filters appeared complex and not very significant, probably because in order to have appreciable quantities of analytes, it would have been more appropriate to use a larger boiler or sample for longer. In any case, it was chosen to consider the sum of the sugars in the filter. The authors observed that the $K_{average}/\sum_{Sugars}$ ratio shows indicative values that are very different between the day in which the boiler was off and the two following days in which the biomass was burned (Table 7).

Table 7. Potassium and total sugar ratios detected during outdoor sampling.

Day	Total Sugars [mg/Nm^3]	K [g/Nm^3]	K/$\sum_{Sugars}$ [g/mg]
1	0.015	386.99	26.55
2	0.026	207.83	8.07
3	0.007	64.05	9.80

The results could suggest a characteristic correlation pattern between the two main biomass combustion markers (sugars and K). Although the tests refer to a limited number of days (1 day of the boiler being off and 2 days of the boiler in operation), it seems clear that a ratio of about 8–9 is indicative of a particulate produced by the combustion of biomass in the boiler, while a ratio of about 26 is indicative of standard environmental conditions. This ratio, obtained at the emissive source (chimney), is 6.75. Since the relationship between these two BB markers is being theorized in this article for the first time, there are no data in the literature to compare with. This ratio is influenced by the fact that K is a BB marker but not a unique one, as it is already present in the atmosphere, while sugars (especially Levoglucosan, mannosan, and galactose) are unique markers of BB.

3.2.4. PM Emission

As regards the sampling of PM, for both tests, considering the biomass burned with and without abatement systems, the PM$_{2.5}$ component is always dominant in the com-

bustion fumes. The tests with the CREA-IT boiler GSA80 in the open burning condition show a higher presence of PM in the combustion fumes, with concentrations of $PM_{2.5}$ of 170.2 mg/Nm^3 (Table 8), approximately twice as many as those observed with the multiple cyclone scrubber (Table 9).

Table 8. PM fractions from CREA-IT boiler in absence of abatement system simulating "open burning".

PM Fractions	Citrus Pruning [mg/Nm^3]	Citrus Pruning [% *w/w*?]
PM_{10}	5.3	2.5
$2.5 < PM < 10$	38.5	18.0
$PM_{2.5}$	170.2	79.5

Table 9. PM fractions from ARSAC with multicylone scrubber as abatement system.

PM Fractions	Citrus Pruning [mg/Nm^3]	Citrus Pruning [% *w/w*?]
PM_{10}	0.95	1.48
$2.5 < PM < 10$	2.39	3.73
$PM_{2.5}$	61.06	94.79

The data obtained regarding the PM fraction distributions from citrus pruning combustion by the two different systems (Tables 8 and 9) show a general decrease in the overall PM concentrations in the fumes when the multicyclone is used. The presence of the filtering system leads to a higher coarser PM abatement respect to $PM_{2.5}$, which, in turn, increases its percentage.

As can be deduced from the TSP results shown in Table 10, open burning produces more PM. In fact, the sum of the PM fractions in Tables 8 and 9 is different based on the data reported in Table 10. One explanation for this difference is due to the type of sampling: the PTS sampling is continuous, while the PM fractions were sampled for time intervals (15 min). This inevitably influenced the sampling and the relative averages obtained. The other reason is gravimetric; in the case of the calculation of the PTS, obviously, the relative error for the filter weighing is referred to a single filter, while in the case of the PM fractions, the weight measurements are related to three different filters, which multiplies the relative errors of the weighings. From the filters' gravimetric measurements of the outdoor autosamplers A, B, C, and D, it was possible to compose distribution maps of PM_{10} in the studied area (Figure 8). During the first day (Figure 8 (left)) with the boiler off, the ambient air autosamplers were in continuous operation from 13:00 to 10:00 the next day. In this phase, despite the inactivity of the boiler, the highest values of PM_{10} per m^3 of sampled volume are observed due to the greater stability conditions at night, which favored the fall of the particulate present in the atmosphere. A significant contribution to the PM concentration on the first sampling day (with the boiler off, Sunday) could be attributable to vehicular traffic from the highway less than one km away from the sampling point. In the following days, with the boiler on, the autosamplers were active only during the day, when winds with greater intensity were recorded. On the third day (Figure 8 (right)), lower concentrations of PM were reported, possibly due to the shorter operating time of the boiler and higher wind speeds, which transported the PM to outside of the studied area. A comparison with local meteorological variables (Table 11) was made possible thanks to the weather station on the ARSAC site. The anemometer was not functional, and the neighboring stations of Acri (WGS84; 16.404836 east; 39.502161 north) and Corigliano Calabro (WGS84; 16.448522 east; 39.736805 north) were taken into consideration for the wind data alone. As mentioned, the north–north/west wind direction during the night of the first day was predominant in the distribution of the PM. The map shows a greater concentration in the autosampler C located to the south. During the second day (Figure 8 (center)), the anemometers in the reference stations detected variable origins and dynamics in the winds, with predominant north–north/west–south/West directions,

which led to a distribution of the PM along the north–south axis. On that day, during the sampling, near station A (north), an agricultural machine had begun plowing, which meant that sampling had to be promptly suspended. This phenomenon may have influenced the sampling at point A, increasing the PM concentration. Finally, regarding the last day (Figure 8 (right)), the winds from north–north/west led to a higher concentration of PM in the south–south/east area. The following figure and table show the PM_{10} distribution maps and the meteorological values recorded during the sampling days, respectively.

Table 10. Total Suspended Particles.

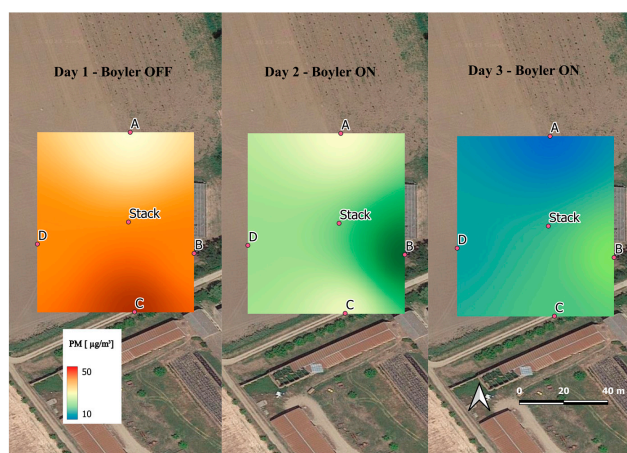| TSP	Open Burning [mg/Nm^3]	Boiler with Abatement System [mg/Nm^3]
PM	103.05	83.10

Figure 8. PM_{10} distribution maps. First day—**left**; second day—**center**; third day—**right**.

Table 11. Meteorological values.

Sampling Period	Air Temperature [°C]	Precipitations [mm]	Moisture [%]	Soil Temperature [°C]	Wind Direction
4th October 2020					
Day	27.8	0	43.09	20.58	NW
Night	18.73	0	77.9	20.92	NW
5th October 2020					
Day	26.04	0	48.28	20.62	NW—SW
Night	22	0	62.4	20.9	SW—N
6th October 2020					
Day	24.29	0	54.42	20.82	NW
Night	19.13	0	65.8	20.98	SW

3.2.5. Metal Emission

The results about the metal contents in the emissions obtained from metal sampling at the stack were divided for the PM filter, the impingers with $H_2O_2 + HNO_3$, and the backup impinger. The results are shown in Table 12.

Table 12. Metal contents in emissions.

Citrus pruning combustion in boiler with abatement system										
[mg/Nm^3]	**Na**	**Mg**	**Al**	**K**	**Ca**	**Cr**	**Mn**	**Fe**	**Ni**	**Cu**
PM filter	5.50	0.73	3.59	110.10	0.99	0.01	0.10	1.78	3×10^{-3}	0.05
Impingers	0.89	0.26	0.42	1.76	1.23	1×10^{-3}	0.01	0.30	6×10^{-3}	0.05
Backup	0.03	0.02	0.04	0.03	0.02	<LOQ	8×10^{-4}	0.04	1×10^{-4}	3×10^{-3}
[mg/Nm^3]	**Zn**	**Ga**	**Sr**	**Ag**	**Cd**	**In**	**Ba**	**Tl**	**Pb**	**Bi**
PM filter	0.33	6×10^{-3}	0.06	5×10^{-4}	3×10^{-4}	1×10^{-4}	0.07	1×10^{-3}	0.07	0.18

Table 12. *Cont.*

Citrus pruning combustion in boiler with abatement system									
Impingers	0.31	3×10^{-4}	0.02	4×10^{-5}	3×10^{-3}	<LOQ	0.01	7×10^{-4}	0.03	2×10^{-3}
Backup	0.01	<LOQ	4×10^{-4}	<LOQ	5×10^{-3}	<LOQ	3×10^{-3}	2×10^{-5}	0.06	<LOQ

Citrus pruning combustion in boiler without abatement system (Open Burning)									
[mg/Nm^3]	**Na**	**Mg**	**Al**	**K**	**Ca**	**Cr**	**Mn**	**Fe**	**Ni**	**Cu**
PM filter	4.00	1.86	4.51	351.90	1.05	0.06	0.23	2.78	9E-04	2E-03
Impingers	1.20	0.55	0.73	0.74	1.66	0.04	0.02	0.89	0.03	0.02
Backup	0.62	0.29	0.38	0.38	0.85	0.02	0.01	0.45	0.01	0.01

[mg/Nm^3]	**Zn**	**Ga**	**Sr**	**Ag**	**Cd**	**In**	**Ba**	**Tl**	**Pb**	**Bi**
PM filter	0.01	1×10^{-3}	0.03	3×10^{-3}	4×10^{-4}	5×10^{-5}	9×10^{-4}	2×10^{-3}	2×10^{-5}	0.02
Impingers	0.17	3×10^{-3}	0.01	0.09	5×10^{-5}	<LOQ	4×10^{-4}	3×10^{-3}	<LOQ	<LOQ
Backup	0.09	1×10^{-3}	2×10^{-3}	0.05	3×10^{-3}	<LOQ	2×10^{-4}	1×10^{-3}	<LOQ	<LOQ

The results show very high concentrations of K distributed almost exclusively on the PM filter, while Na, Mg, and Ca show a different trend; in fact, they were found to be present also in the volatile fraction collected in the impingers.

The use of the multicyclone resulted in a strong reduction in the metals released into the atmosphere. In fact, they are often transported by the PM, which facilitates the transport; therefore, in the tests with the multicyclone, we noted negligible concentrations in the backup bubbler. Cd and the Pb show a different behavior, with high concentrations being detected in the backup bubblers by virtue of their high volatility. These data are more recognizable in Figure 9, which represents the values listed in Table 12 as percentages of the distribution.
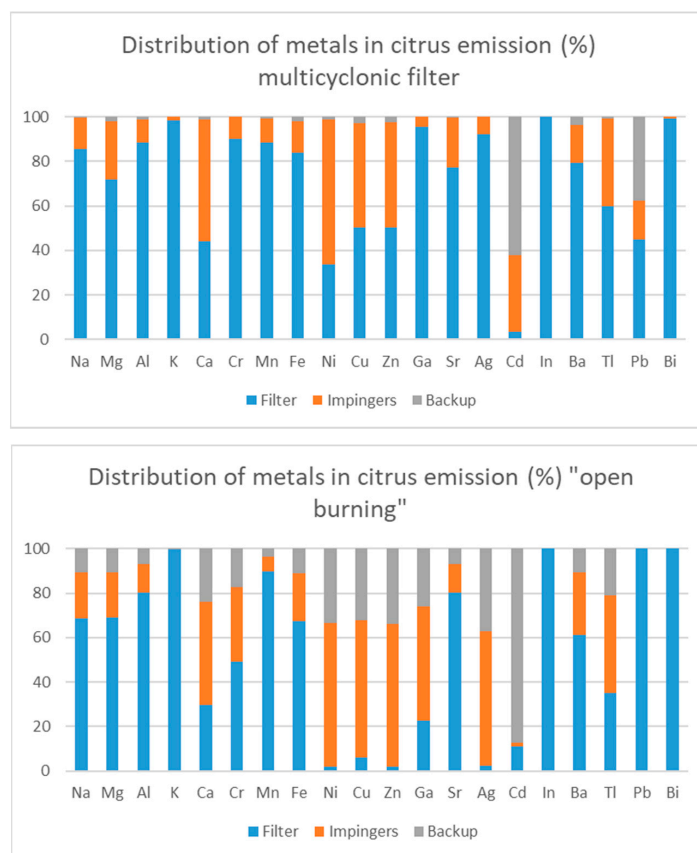

Figure 9. The distribution of the metals in the emissions from citrus pruning combustion in a boiler equipped with a multicyclonic filter (**above**) and without any filter in "open burning" conditions (**down**).

The values of the metals obtained from environmental sampling in the various sites on the various days are reported in Table 13.

Table 13. Metal concentrations in environmental sites A, B, C, and D.

[ng/Nm^3]	Na	Mg	Al	K	Ca	Cr	Mn	Fe	Ni	Cu
A1	747.30	152.40	1.51	489.987	109.70	0.10	2.12	1.84	0.23	0.48
A2	867.27	199.42	2.38	344.55	175.05	0.13	3.11	2.71	0.34	0.71
A3	504.30	72.76	0.19	107.73	10.38	0.05	0.56	0.47	0.06	0.12
B1	1122.17	226.48	25.18	301.16	362.76	0.13	9.76	8.37	0.29	1.22
B2	681.73	126.88	1.48	103.37	100.53	0.11	3.10	2.50	0.19	0.03
B3	1105.50	106.60	0.23	63.65	16.32	0.05	0.81	0.03	0.07	0.07
C1	4608.35	404.65	19.81	397.91	461.84	0.13	10.42	8.67	0.52	2.06
C2	1494.04	204.44	11.54	220.74	187.15	0.18	4.84	6.14	0.15	0.13
C3	612.26	87.54	0.31	49.73	12.39	0.05	0.61	0.38	0.10	0.07
D1	1584.62	254.87	42.64	358.89	406.57	0.08	11.64	14.10	0.34	1.24
D2	772.96	146.87	13.59	162.67	129.55	0.07	4.13	3.36	0.14	0.12
D3	403.49	57.25	0.42	35.07	7.20	0.01	0.32	<LOQ	0.08	0.18

[ng/Nm^3]	Zn	Ga	Sr	Ag	Cd	In	Ba	Tl	Pb	Bi
A1	11.41	0.09	5.56	0.01	0.39	0.05	1.76	0.00	0.56	0.22
A2	16.55	0.15	8.88	0.02	0.58	0.07	2.84	0.01	0.81	0.34
A3	3.29	0.01	0.51	0.00	0.09	0.01	0.14	0.00	0.15	0.04
B1	3.21	0.12	10.34	<LOQ	0.10	0.00	2.51	0.14	0.27	0.03
B2	3.13	0.03	3.71	<LOQ	<LOQ	0.00	0.91	0.01	0.10	0.00
B3	1.67	0.01	0.80	0.00	<LOQ	<LOQ	0.18	0.01	0.03	0.01
C1	12.70	0.16	16.41	<LOQ	<LOQ	<LOQ	3.66	0.16	0.23	0.00
C2	4.90	0.07	7.35	0.02	<LOQ	<LOQ	1.79	0.05	0.14	<LOQ
C3	3.35	0.01	0.73	0.00	<LOQ	<LOQ	0.23	0.01	0.02	<LOQ
D1	2.95	0.17	11.81	0.00	<LOQ	<LOQ	3.73	0.20	0.30	<LOQ
D2	5.05	0.08	5.74	0.02	<LOQ	<LOQ	1.87	0.03	0.08	<LOQ
D3	2.54	0.00	0.43	0.01	<LOQ	<LOQ	0.18	0.01	0.04	<LOQ

4. Conclusions

This paper reports the results of a comparison between the emissions produced by the combustion of biomass in a boiler without an abatement system (simulating open burning) and that in a boiler with a multicyclonic abatement system. In the second case, atmospheric PM_{10} monitoring stations were also installed at a radius of about 40 m from the emissive source (stack).

Regarding macropollutants (CO, CO_2, NO_x, SO_2, TOC), there were profound differences that indicate how combustion in "open burning" took place under worse oxidizer supply conditions, with the concentration of CO being about twice as high as that of the other tests in the boiler. The concentration of NO_x was also higher in the "open burning" tests, where it was therefore deduced that higher temperatures were reached. Only the concentration of SO_2 is similar in both cases. As regards the emitted PM, it is obvious that the presence of the multicyclone filter has a positive effect on emissions and reduces the atmospheric impact. This effect, however, is closely related to the size of the particulates, and the abatement system gradually becomes less effective since the aerodynamic diameter of the PM considered decreases. PM sampling on the surrounding area showed higher concentrations even in the day before testing, showing that a boiler with an effective abatement system did not adversely affect the atmosphere. The sampling of the sugars in the chimney and the environmental filters showed how open burning leads to the production of a higher number of markers and with higher concentrations. It has been noted that there seems to be a characteristic ratio on atmospheric sampling between K(g/Nm^3) and $\sum_{Sugars}$ (mg/Nm^3); this ratio, in fact, seems to be about 26 under standard conditions, while it is about 8–9 in the area surrounding combustion. At the chimney, this ratio drops to 6.75. This comprehensive study represents a significant step forward in our quest for a more thor-

ough comprehension of air pollution dynamics, particularly concerning the contribution of biomass plants. By meticulously examining the emissions generated by these facilities, this research discerns their unique impact on air quality amidst the complex interplay of various sources. Through sophisticated analysis and data interpretation, it enables us to disentangle the specific pollutants attributable to biomass combustion from those originating from distinct sources like vehicular emissions or residential heating activities.

A crucial aspect facilitating this attribution is the thorough sampling and analysis of the levoglucosan marker. Levoglucosan provides a comprehensive view of the emissions produced at the biomass plant without underestimation, which can occur in ambient sampling, wherein levoglucosan tends to degrade in the atmosphere. This meticulous approach ensures a more accurate assessment of biomass plant emissions and their environmental impact.

Such granular insights are invaluable for crafting targeted policies and interventions aimed at mitigating air pollution hotspots and safeguarding public health and environmental integrity. Ultimately, this study lays a crucial foundation for informed decision-making and sustainable management practices in our ongoing battle against air pollution.

References

1. Maschio, S.; Tonello, G.; Piani, L.; Furlani, E. Fly and Bottom Ashes from Biomass Combustion as Cement Replacing Components in Mortars Production: Rheological Behaviour of the Pastes and Materials Compression Strength. *Chemosphere* **2011**, *85*, 666–671. [CrossRef] [PubMed]
2. Crutzen, P.J.; Heidt, L.E.; Krasnec, J.P.; Pollock, W.H.; Seiler, W. Biomass Burning as a Source of Atmospheric Gases CO, H_2, N_2O, NO, CH_3Cl and COS. *Nature* **1979**, *282*, 253–256. [CrossRef]
3. Lemieux, P.M.; Lutes, C.C.; Santoianni, D.A. Emissions of Organic Air Toxics from Open Burning: A Comprehensive Review. *Prog. Energy Combust. Sci.* **2004**, *30*, 1–32. [CrossRef]
4. Urbanski, S.P.; Hao, W.M.; Nordgren, B. The Wildland Fire Emission Inventory: Western United States Emission Estimates and an Evaluation of Uncertainty. *Atmos. Chem. Phys.* **2011**, *11*, 12973–13000. [CrossRef]
5. Hobbs, P.V.; Sinha, P.; Yokelson, R.J.; Christian, T.J.; Blake, D.R.; Gao, S.; Kirchstetter, T.W.; Novakov, T.; Pilewskie, P. Evolution of Gases and Particles from a Savanna Fire in South Africa. *J. Geophys. Res. Atmos.* **2003**, *108*, 8485. [CrossRef]
6. Rosenfeld, D. TRMM Observed First Direct Evidence of Smoke from Forest Fires Inhibiting Rainfall. *Geophys. Res. Lett.* **1999**, *26*, 3105–3108. [CrossRef]
7. Van Der Werf, G.R.; Randerson, J.T.; Giglio, L.; Collatz, G.J.; Mu, M.; Kasibhatla, P.S.; Morton, D.C.; Defries, R.S.; Jin, Y.; Van Leeuwen, T.T. Global Fire Emissions and the Contribution of Deforestation, Savanna, Forest, Agricultural, and Peat Fires (1997–2009). *Atmos. Chem. Phys.* **2010**, *10*, 11707–11735. [CrossRef]

8. Paris, E.; Carnevale, M.; Vincenti, B.; Palma, A.; Guerriero, E.; Borello, D.; Gallucci, F. Evaluation of VOCs Emitted from Biomass Combustion in a Small CHP Plant: Difference between Dry and Wet Poplar Woodchips. *Molecules* **2022**, *27*, 955. [CrossRef] [PubMed]

9. Andreae, M.O.; Merlet, P. Emission of Trace Gases and Aerosols from Biomass Burning. *Glob. Biogeochem. Cycles* **2001**, *15*, 955–966. [CrossRef]

10. Marlier, M.E.; Defries, R.S.; Voulgarakis, A.; Kinney, P.L.; Randerson, J.T.; Shindell, D.T.; Chen, Y.; Faluvegi, G. El Niño and Health Risks from Landscape Fire Emissions in Southeast Asia. *Nat. Clim. Chang.* **2013**, *3*, 131–136. [CrossRef]

11. Vallero, D.A. *Fundamentals of Air Pollution*; Elsevier Inc.: Amsterdam, The Netherlands, 2007; ISBN 9780123736154.

12. Migo-Sumagang, M.V.P.; Van Hung, N.; Detras, M.C.M.; Alfafara, C.G.; Borines, M.G.; Capunitan, J.A.; Gummert, M. Optimization of a Downdraft Furnace for Rice Straw-Based Heat Generation. *Renew. Energy* **2020**, *148*, 953–963. [CrossRef]

13. Mason, S.A.; Field, R.J.; Yokelson, R.J.; Kochivar, M.A.; Tinsley, M.R.; Ward, D.E.; Hao, W.M. Complex Effects Arising in Smoke Plume Simulations Due to Inclusion of Direct Emissions of Oxygenated Organic Species from Biomass Combustion. *J. Geophys. Res. Atmos.* **2001**, *106*, 12527–12539. [CrossRef]

14. Ward, D.S.; Kloster, S.; Mahowald, N.M.; Rogers, B.M.; Randerson, J.T.; Hess, P.G. The Changing Radiative Forcing of Fires: Global Model Estimates for Past, Present and Future. *Atmos. Chem. Phys.* **2012**, *12*, 10857–10886. [CrossRef]

15. Campos Braga, R.; Rosenfeld, D.; Weigel, R.; Jurkat, T.; Andreae, M.O.; Wendisch, M.; Pöschl, U.; Voigt, C.; Mahnke, C.; Borrmann, S.; et al. Further Evidence for CCN Aerosol Concentrations Determining the Height of Warm Rain and Ice Initiation in Convective Clouds over the Amazon Basin. *Atmos. Chem. Phys.* **2017**, *17*, 14433–14456. [CrossRef]

16. Cecchini, M.A.; MacHado, L.A.T.; Andreae, M.O.; Martin, S.T.; Albrecht, R.I.; Artaxo, P.; Barbosa, H.M.J.; Borrmann, S.; Fütterer, D.; Jurkat, T.; et al. Sensitivities of Amazonian Clouds to Aerosols and Updraft Speed. *Atmos. Chem. Phys.* **2017**, *17*, 10037–10050. [CrossRef]

17. Hamilton, D.S.; Hantson, S.; Scott, C.E.; Kaplan, J.O.; Pringle, K.J.; Nieradzik, L.P.; Rap, A.; Folberth, G.A.; Spracklen, D.V.; Carslaw, K.S. Reassessment of Pre-Industrial Fire Emissions Strongly Affects Anthropogenic Aerosol Forcing. *Nat. Commun.* **2018**, *9*, 3182. [CrossRef]

18. Thornhill, G.D.; Ryder, C.L.; Highwood, E.J.; Shaffrey, L.C.; Johnson, B.T. The Effect of South American Biomass Burning Aerosol Emissions on the Regional Climate. *Atmos. Chem. Phys.* **2018**, *18*, 5321–5342. [CrossRef]

19. Wiedinmyer, C.; Akagi, S.K.; Yokelson, R.J.; Emmons, L.K.; Al-Saadi, J.A.; Orlando, J.J.; Soja, A.J. The Fire INventory from NCAR (FINN): A High Resolution Global Model to Estimate the Emissions from Open Burning. *Geosci. Model Dev.* **2011**, *4*, 625–641. [CrossRef]

20. Guenther, A.; Karl, T.; Harley, P.; Wiedinmyer, C.; Palmer, P.I.; Geron, C. Estimates of Global Terrestrial Isoprene Emissions Using MEGAN (Model of Emissions of Gases and Aerosols from Nature). *Atmos. Chem. Phys.* **2006**, *6*, 3181–3210. [CrossRef]

21. Bond, T.C.; Streets, D.G.; Yarber, K.F.; Nelson, S.M.; Woo, J.H.; Klimont, Z. A Technology-Based Global Inventory of Black and Organic Carbon Emissions from Combustion. *J. Geophys. Res. Atmos.* **2004**, *109*, 1–43. [CrossRef]

22. Nussbaumer, T.; Braun, C.; Burtscher, H.; Livbjerg, H.; Jokiniemi, J.; Ebert, F.; Tullin, C.; Baxter, L.L.; Ehrlich, C.; Oser, M.; et al. *Aerosols from Biomass Combustion*; IEA Bioenergy: Paris, France, 2001; ISBN 3908705002.

23. Chen, H.; Yin, S.; Li, X.; Wang, J.; Zhang, R. Analyses of Biomass Burning Contribution to Aerosol in Zhengzhou during Wheat Harvest Season in 2015. *Atmos. Res.* **2018**, *207*, 62–73. [CrossRef]

24. Wan, X.; Kang, S.; Li, Q.; Rupakheti, D.; Zhang, Q.; Guo, J.; Chen, P.; Tripathee, L.; Rupakheti, M.; Panday, A.K.; et al. Organic Molecular Tracers in the Atmospheric Aerosols from Lumbini, Nepal, in the Northern Indo-Gangetic Plain: Influence of Biomass Burning. *Atmos. Chem. Phys.* **2017**, *17*, 8867–8885. [CrossRef]

25. Zhang, Y.; Obrist, D.; Zielinska, B.; Gertler, A. Particulate Emissions from Different Types of Biomass Burning. *Atmos. Environ.* **2013**, *72*, 27–35. [CrossRef]

26. Saarnio, K.; Teinilä, K.; Aurela, M.; Timonen, H.; Hillamo, R. High-Performance Anion-Exchange Chromatography–Mass Spectrometry Method for Determination of Levoglucosan, Mannosan, and Galactosan in Atmospheric Fine Particulate Matter. *Anal. Bioanal. Chem.* **2010**, *398*, 2253–2264. [CrossRef] [PubMed]

27. Saarnio, K.; Teinilä, K.; Saarikoski, S.; Carbone, S.; Gilardoni, S.; Timonen, H.; Aurela, M.; Hillamo, R. Online Determination of Levoglucosan in Ambient Aerosols with Particle-into-Liquid Sampler – High-Performance Anion-Exchange Chromatography – Mass Spectrometry (PILS-HPAEC-MS). *Atmos. Meas. Tech.* **2013**, *6*, 2839–2849. [CrossRef]

28. Vincenti, B.; Paris, E.; Carnevale, M.; Palma, A.; Guerriero, E.; Borello, D.; Paolini, V.; Gallucci, F. Saccharides as Particulate Matter Tracers of Biomass Burning: A Review. *Int. J. Environ. Res. Public Health* **2022**, *19*, 4387. [CrossRef]

29. Puxbaum, H.; Caseiro, A.; Sánchez-Ochoa, A.; Kasper-Giebl, A.; Claeys, M.; Gelencsér, A.; Legrand, M.; Preunkert, S.; Pio, C.A. Levoglucosan Levels at Background Sites in Europe for Assessing the Impact of Biomass Combustion on the European Aerosol Background. *J. Geophys. Res. Atmos.* **2007**, *112*, D23S05. [CrossRef]

30. Schkolnik, G.; Rudich, Y. Detection and Quantification of Levoglucosan in Atmospheric Aerosols: A Review. *Anal. Bioanal. Chem.* **2006**, *385*, 26–33. [CrossRef] [PubMed]

31. Caseiro, A.; Marr, I.L.; Claeys, M.; Kasper-Giebl, A.; Puxbaum, H.; Pio, C.A. Determination of Saccharides in Atmospheric Aerosol Using Anion-Exchange High-Performance Liquid Chromatography and Pulsed-Amperometric Detection. *J. Chromatogr. A* **2007**, *1171*, 37–45. [CrossRef]

32. Piot, C.; Jaffrezo, J.L.; Cozic, J.; Pissot, N.; El Haddad, I.; Marchand, N.; Besombes, J.L. Quantification of Levoglucosan and Its Isomers by High Performance Liquid Chromatography-Electrospray Ionization Tandem Mass Spectrometry and Its Applications to Atmospheric and Soil Samples. *Atmos. Meas. Tech.* **2012**, *5*, 141–148. [CrossRef]

33. Giannoni, M.; Martellini, T.; Del Bubba, M.; Gambaro, A.; Zangrando, R.; Chiari, M.; Lepri, L.; Cincinelli, A. The Use of Levoglucosan for Tracing Biomass Burning in PM2.5 Samples in Tuscany (Italy). *Environ. Pollut.* **2012**, *167*, 7–15. [CrossRef]

34. Yan, C.; Zheng, M.; Sullivan, A.P.; Shen, G.; Chen, Y.; Wang, S.; Zhao, B.; Cai, S.; Desyaterik, Y.; Li, X.; et al. Residential Coal Combustion as a Source of Levoglucosan in China. *Environ. Sci. Technol.* **2018**, *52*, 1665–1674. [CrossRef] [PubMed]

35. Sheesley, R.J.; Mieritz, M.; DeMinter, J.T.; Shelton, B.R.; Schauer, J.J. Development of an In Situ Derivatization Technique for Rapid Analysis of Levoglucosan and Polar Compounds in Atmospheric Organic Aerosol. *Atmos. Environ.* **2015**, *123*, 251–255. [CrossRef]

36. Paris, E.; Carnevale, M.; Guerriero, E.; Palma, A.; Vincenti, B.; Khalid, A.; Rantica, E.; Proto, A.R.; Gallucci, F. Fixed Source Monitoring System for Marker Emission During Biomass Combustion. *SSRN Electron. J.* **2022**, *208*, 597–603. [CrossRef]

37. Dai, J.; Grace, J.R. Biomass Screw Feeding with Tapered and Extended Sections. *Powder Technol.* **2008**, *186*, 56–64. [CrossRef]

38. Dai, J.; Cui, H.; Grace, J.R. Biomass Feeding for Thermochemical Reactors. *Prog. Energy Combust. Sci.* **2012**, *38*, 716–736. [CrossRef]

39. Colantoni, A.; Paris, E.; Bianchini, L.; Ferri, S.; Marcantonio, V.; Carnevale, M.; Palma, A.; Civitarese, V.; Gallucci, F. Spent Coffee Ground Characterization, Pelletization Test and Emissions Assessment in the Combustion Process. *Sci. Rep.* **2021**, *11*, 5199. [CrossRef] [PubMed]

40. Proto, A.R.; Palma, A.; Paris, E.; Papandrea, S.F.; Vincenti, B.; Carnevale, M.; Guerriero, E.; Bonofiglio, R.; Gallucci, F. Assessment of Wood Chip Combustion and Emission Behavior of Different Agricultural Biomasses. *Fuel* **2021**, *289*, 119758. [CrossRef]

41. Paris, E.; Gallucci, F.; Carnevale, M.; Khalid, A.; Paolini, V.; Guerriero, E. Evaluation of the Vocs Emitted by the Combustion of Rice Straw. In Proceedings of the European Biomass Conference and Exhibition Proceedings, Lisbon, Portugal, 27–30 May 2019.

42. Paris, E.; Avino, P.; Guerriero, E.; Vincenti, B.; Palma, A.; Carnevale, M.; Benedetti, P.; Torre, M.; Gallucci, F. Activated Porous Carbon Fiber: New Adsorbent for Sampling and Analysis by Thermal Desorption of Siloxanes in Biogas and Biomethane. *Int. J. Environ. Res. Public Health* **2022**, *19*, 10890. [CrossRef]

43. Chu, D.; Xue, L.; Zhang, Y.; Kang, L.; Mu, J. Surface Characteristics of Poplar Wood with High-Temperature Heat Treatment: Wettability and Surface Brittleness. *Bioresources* **2016**, *11*, 6948–6967. [CrossRef]

44. Gallucci, F.; Pari, L.; Longo, L.; Carnevale, M.; Santangelo, E.; Colantoni, A.; Paolini, V.; Guerriero, E.; Tonolo, A. Assessment of Organic Micropollutants (Pcdd/Fs and Pcbs) from Biomass Combustion in a Small Chp Facility. In Proceedings of the European Biomass Conference and Exhibition Proceedings, ETA-Florence Renewable Energies. Copenhagen, Denmark, 14–18 May 2018; Volume 2018, pp. 606–609.

45. Carnevale, M.; Paris, E.; Palma, A.; Vincenti, B.; Salerno, M.; Manganiello, R.; Guerriero, E.; Perilli, M.; Colantoni, A.; Proto, A.R.; et al. Characterization of Emissions from Combustion of Olive Wood Chips. In Proceedings of the European Biomass Conference and Exhibition Proceedings, Online, 26–29 April 2021; pp. 577–580.

46. Vassilev, S.V.; Baxter, D.; Andersen, L.K.; Vassileva, C.G.; Morgan, T.J. An Overview of the Organic and Inorganic Phase Composition of Biomass. *Fuel* **2012**, *94*, 1–33. [CrossRef]

47. Arvelakis, S.; Gehrmann, H.; Beckmann, M.; Koukios, E.G. Effect of Leaching on the Ash Behavior of Olive Residue during Fluidized Bed Gasification. *Biomass Bioenergy* **2002**, *22*, 55–69. [CrossRef]

48. Glarborg, P.; Miller, J.A.; Ruscic, B.; Klippenstein, S.J. Modeling Nitrogen Chemistry in Combustion. *Prog. Energy Combust. Sci.* **2018**, *67*, 31–68. [CrossRef]

49. Zdráhal, Z.; Oliveira, J.; Vermeylen, R.; Claeys, M.; Maenhaut, W. Improved Method for Quantifying Levoglucosan and Related Monosaccharide Anhydrides in Atmospheric Aerosols and Application to Samples from Urban and Tropical Locations. *Environ. Sci. Technol.* **2002**, *36*, 747–753. [CrossRef]

50. Simoneit, B.R.T.; Elias, V.O. Detecting Organic Tracers from Biomass Burning in the Atmosphere. *Mar. Pollut. Bull.* **2001**, *42*, 805–810. [CrossRef]

51. Fraser, M.P.; Lakshmanan, K. Using Levoglucosan as a Molecular Marker for the Long-Range Transport of Biomass Combustion Aerosols. *Environ. Sci. Technol.* **2000**, *34*, 4560–4564. [CrossRef]

52. Simoneit, B.R.T.; Schauer, J.J.; Nolte, C.G.; Oros, D.R.; Elias, V.O.; Fraser, M.P.; Rogge, W.F.; Cass, G.R. Levoglucosan, a Tracer for Cellulose in Biomass Burning and Atmospheric Particles. *Atmos. Environ.* **1999**, *33*, 173–182. [CrossRef]